On the scaling properties of the total γ^*p cross section

Miguel N. Mondragon, J.G. Contreras*
Departamento de Física Aplicada,
Centro de Investigación y Estudios Avanzados del I.P.N.,
97310, Mérida, Yucatán, México.

Abstract

We perform a detailed analysis on the scaling properties of the total γ^*p cross section, $\sigma_{\gamma^*\mathrm{p}}$. We write the cross section as a product of two functions W and V representing, respectively, the dynamical degrees of freedom and the contribution from the valence partons. Analyzing data from HERA and fixed target experiments we find that V is nearly independent of Q^2 and concentrated at large x, while W carries all the information on the Q^2 evolution of γ^*p. We define the reduced cross section $\tilde{\sigma}_{\gamma^*\mathrm{p}} \equiv W = \sigma_{\gamma^*\mathrm{p}}/V$, and show that it is very close to a generalized homogeneous function. This property gives rise to geometric scaling not only for small x, but for all the current measured kinematic plane. As a consequence of our *Ansatz* we also obtain a compact parameterization of $\sigma_{\gamma^*\mathrm{p}}$ describing all data above $Q^2 = 1$ GeV^2.

1 Introduction

It has been found that for low values of the Bjorken variable x, $x \leq 0.01$, the total γ^*p cross section, $\sigma_{\gamma^*\mathrm{p}}(x, Q^2)$, extracted from lepton–hadron scattering presents the property of geometric scaling [1, 2]. This property permits to write the cross section as a function of only one variable, τ, called the scaling variable, which is the product of two functions, one depending only on Q^2 and the other only on x. It has been suggested that, for $\sigma_{\gamma^*\mathrm{p}}$, τ is given by Q^2/Q_s^2 with $Q_s^2 = Q_s^2(x)$ known as the saturation scale. Geometric scaling has also been observed in eA reactions [3], inclusive charm production [4] and nucleus–nucleus collisions [5].

The observation that $\sigma_{\gamma^*\mathrm{p}}$ grows quite rapidly at low x and that this behavior can not continue indefinitely without violating the unitarity of the cross section

---

*Corresponding author. E–mail: jgcn@mda.cinvestav.mx

led to the proposal of nonlinear QCD equations containing saturation [6, 7, 8, 9, 10, 11]. One of the features of this type of equations is the introduction of a scale, Q_s^2, to signal the onset of saturation effects. Much of the excitement and advance in the understanding of perturbative QCD at low x in recent years comes from the discovery that some saturation equations imply geometric scaling at the saturation scale [12, 13, 14, 15].

Much recent theoretical work has been devoted to find both, the region where geometric scaling is valid and the functional form of the violations to geometric scaling above the saturation scale. Studies based on the BFKL equation [16] supplemented with specific boundary conditions have found that there is a window of phase space above Q_s^2 and below a $Q_{\max}^2$ on which geometric scaling is valid. For current accessible energies, $Q_{\max}^2$ is of the order of 100 GeV^2 [17, 18, 19]. More recently, there have been indications that, in a more general nonlinear equation, geometric scaling is strongly violated [20].

As the concept of geometric scaling has been linked to saturation, none of these investigations expect geometric scaling to be valid at large x where the density of partons is very small.

Here we study in detail the scaling properties of the total γ^*p cross section and find that geometric scaling is related to the fact that at small x, σ_{γ^*p} is very close to a homogeneous function, specifically a power law in both, x and Q^2. We show that it is possible to define a reduced cross section, called $\tilde{\sigma}_{\gamma^*p}$ in the following, which isolates this power law behavior not only for the small, but also for the large x region and thus shows geometric scaling in the complete kinematic plane.

This document is organized as follows. In the next section, we show that it is possible to isolate the power law behavior in x of σ_{γ^*p} for all values of Q^2 and define the reduced cross section $\tilde{\sigma}_{\gamma^*p}$. In Section 3 we study the behavior of $\tilde{\sigma}_{\gamma^*p}$ and show that it is very close to a generalized homogeneous function. In Section 4 we discuss the implications of our findings regarding saturation and geometric scaling. We also present a compact parametrization of σ_{γ^*p} which describes all data above $Q^2 = 1$ GeV^2. Finally, in Section 5 we briefly summarize our findings and present our conclusions.

2   Analysis of the x and Q^2 dependence of σ_{γ^*p}

First, we turn to the behavior of σ_{γ^*p} at small x. It is know, that the experimental data at small x can be described at each value of Q^2 by a power law in x [22]. From the point of view of theory, this behavior is expected, for Q^2 big enough to justify the use of pQCD, from both, the DLLA approximation [23] if the starting Q^2 value for the QCD evolution is taken sufficiently small (see for example [24]), and from the BFKL [16] evolution.

In fact, this behavior is also seen in studies of geometric scaling above the saturation scale. For concreteness we use the saturation scale $Q_s^2(x) \sim x^{-\lambda_{\text{GBW}}}$, with $\lambda_{\text{GBW}} = 0.288$, as defined by K. Golec-Biernat and M. Wüsthoff [21]. Staśto *et al.* [1] found that, for $\tau = Q^2/Q_s^2(x) > 1$, $\sigma_{\gamma^*p}(\tau) \sim 1/\tau$ suggesting a

power law behavior of $\sigma_{\gamma^*\mathrm{p}}$ as a function of x for constant values of Q^2.

In summary, it is expected from theory and phenomenology, and confirmed by experiment that, at small x, $\sigma_{\gamma^*\mathrm{p}}$ behaves as a power law for fixed values of Q^2. Following these results, we propose to write the total $\gamma^*\mathrm{p}$ cross section at each Q^2 value as the product of two functions W and V:

$$\sigma_{\gamma^*\mathrm{p}} = WV \tag{1}$$

where

$$W = N\bar{x}^{-\lambda}, \tag{2}$$

and we use $\bar{x}$ instead of x–Bjorken [21]. Both are related through

$$\bar{x} = x\left(1 + \frac{4m_f^2}{Q^2}\right), \tag{3}$$

with $m_f = 140$ MeV. Note that x and $\bar{x}$ are substantially different only at very low Q^2. Note also that in equation (2) both, the normalization, N, and the exponent of the power law, λ, may be different, for different values of Q^2; i.e., $N = N(Q^2)$ and $\lambda = \lambda(Q^2)$.

As we are interested in isolating the scaling behavior of the cross section we require from V to be approximately constant at small x, so that it does not alter the physics embodied in W, and that it describes the cross section at large x. It turns out that these requirements are very closed to those expected from a valence distribution, so we tried the following functional form inspired in the work of [25, 26]:

$$V = \exp\left(-\frac{(\bar{x} - x_0)^2}{4\sigma^2}\right)\mathrm{erf}\left(\frac{1 - (x - x_0)}{2\sigma}\right), \tag{4}$$

where the Gaussian represents the valence distribution of the proton and the error function takes care of enforcing the different kinematic constrains.

We proceed now to test the *Ansatz* embodied in equations (1–4). We use data from fixed target [27] and HERA [28, 29] experiments. We chose Q^2 values such that there are measurements from both, fixed target and HERA experiments, either at the same or at very similar Q^2. Normally, these Q^2 values are slightly different. We correct the fixed target data to the HERA values using the H1 PDF 2000 fit [28]. In most cases the correction factors are at the per mil level with a few cases at the one and two percent level. We then fit the data to the functional form of equation (1) for each Q^2 value. As an example, Figure 1 shows data from HERA and fixed target experiments at $Q^2=12$ GeV^2 and $Q^2=120$ GeV^2 along with the result of the fit.

The data in Figure 1 is very well described by equation (1). Furthermore, the same can be said at each value of Q^2 where there are measured points from both, fixed target and HERA experiments. Remarkably, we find that x_0 and σ^2 from equation (4) do not depend on Q^2. They take the values $x_0 = 0.27$ and $\sigma^2 = 0.036$.
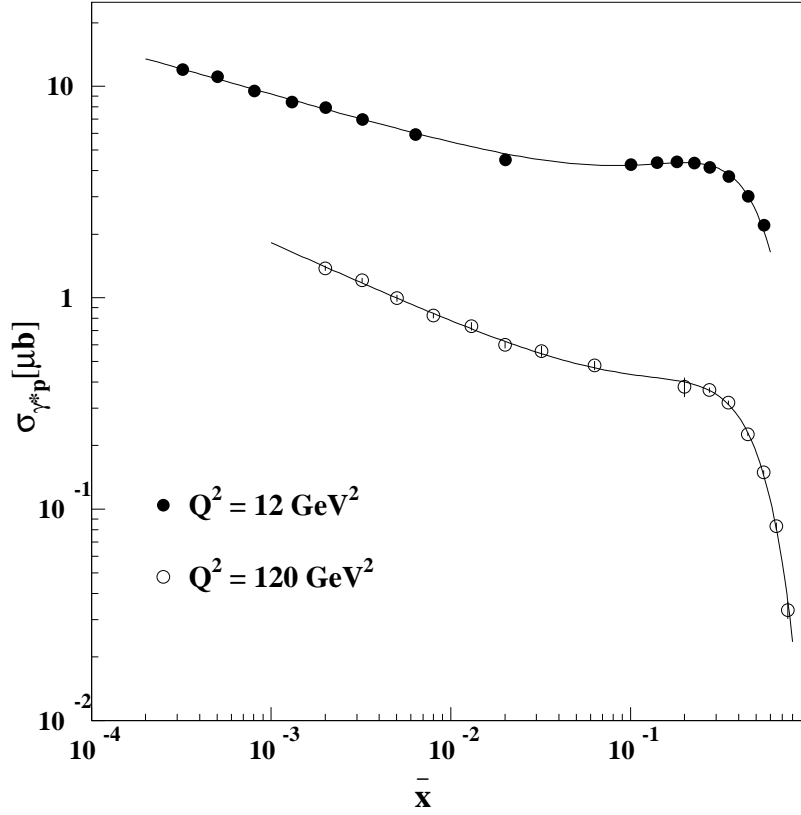
Figure 1: The total γ^*p cross section is shown as a function of $\bar{x}$ for Q^2=12 GeV^2 and Q^2=120 GeV^2 . The points are experimental data from fixed target and HERA experiments and the line is a fit to the form of equations (1–4). A power law is clearly seen at low values of $\bar{x}$, while the structure at high $\bar{x}$ corresponds to a Gaussian–like distribution.

The fact that V is independent of Q^2 implies that all the QCD evolution in Q^2 of the cross section is entirely contained in W. Thus, we define, in the complete kinematic plane, the reduced cross section $\tilde{\sigma}_{\gamma^*\mathrm{p}}$ as

$$\tilde{\sigma}_{\gamma^*\mathrm{p}} \equiv W(x, Q^2) = \sigma_{\gamma^*\mathrm{p}}/V(x). \tag{5}$$

3 Analysis of the behavior of $\tilde{\sigma}_{\gamma^*\mathrm{p}}$

We turn now to study the reduced cross section. Specifically, we study the dependence on Q^2 of both N and λ. We use all HERA data [28, 29] to fit $\tilde{\sigma}_{\gamma^*\mathrm{p}}$ for fixed values of Q^2. We do not use fixed target data at this stage of the analysis, because those data points are concentrated at high x and thus, they do not have a lever arm long enough to determine accurately the power law parameters. Their influence has already been taken into account through $V(x)$.

We use 40 different experimental Q^2 values, ranging from 0.15 to 8000 GeV^2, with enough data points in x to perform the fit. The average number of points for each fit was 8, ranging from 5 to 12. At each value of Q^2, equation (2) provides an excellent description of data. The results for N and λ for each individual fit are quite precise and provide a clear picture of their Q^2 dependence as shown in Figure 2.

We observe a dramatic change in the behavior of both functions, $N(Q^2)$ and $\lambda(Q^2)$, when the virtuality of the photon approaches from above the region below 1 GeV^2. Here λ is, as expected, very similar to the one found with the Donnachie–Landshoff parametrization [30]; while the normalization appears to saturate. Furthermore, the value of N and λ for the Q^2 data below 1 GeV^2 are almost constant in comparison to the steep dependence of these functions above 1 GeV^2.

Above $Q^2 \approx 1$ GeV^2, $\lambda(Q^2)$ can be described with the following functional form

$$\lambda(Q^2) = \alpha \log_{10}(Q^2/\Lambda^2), \tag{6}$$

while $N(Q^2)$ behaves as the power law

$$N(Q^2) = \beta \left(\frac{Q^2}{Q_0^2}\right)^{-(1+\epsilon)}, \tag{7}$$

where Q_0^2 is taken as 1 GeV^2.

A fit in the intermediate Q^2 region to the data plotted in Figure 2 yields $\beta = 41.1 \pm 1.5$ μb, $\epsilon = 0.104 \pm 0.007$, $\alpha = 0.135 \pm 0.003$ and $\Lambda^2 = 0.17 \pm 0.03$ GeV^2. The quality of the fits is $\chi^2/dof = 0.66$ and $\chi^2/dof = 0.33$ for $N(Q^2)$ and $\lambda(Q^2)$ respectively. Note that the points at the largest Q^2 were not taken into account, because they have big fluctuations due to the limited statistics of data.
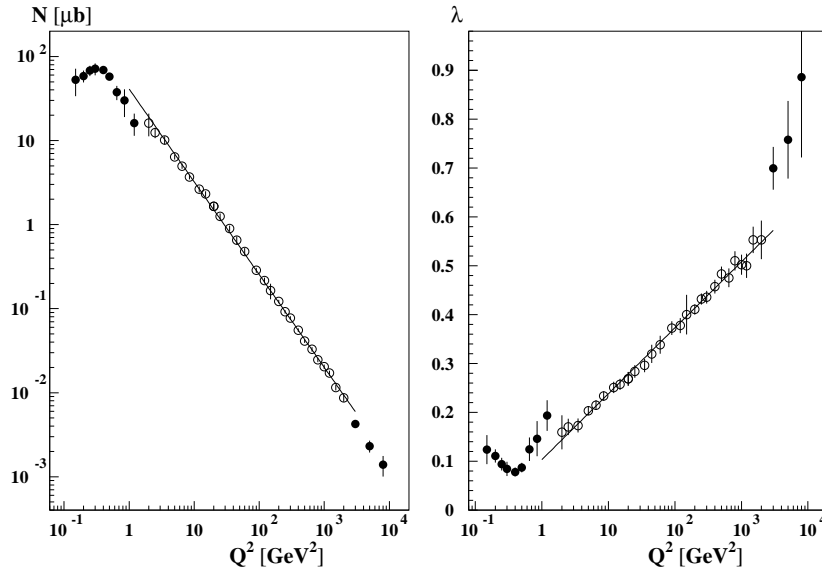
Figure 2: The Q^2 dependence of the normalization N and the exponent λ of $\tilde{\sigma}_{\gamma^*\mathrm{p}} = N\bar{x}^{-\lambda}$, extracted from fits of HERA data to the reduced cross section $\tilde{\sigma}_{\gamma^*\mathrm{p}}$ at fixed values of Q^2. The solid lines are fits to equations (6) and (7) in the intermediate Q^2 range given by the empty bullets in the figure.

In summary, for Q^2 values below 1 GeV^2 the Q^2 dependence of W is very soft and the function depends mainly on one variable: x. Above 1 GeV^2 W is very well described by the following functional form:

$$W(\bar{x}, Q^2) = \beta \left(\frac{Q^2}{Q_0^2}\right)^{-(1+\epsilon)} \bar{x}^{-\alpha \log_{10}(Q^2/\Lambda^2)}. \tag{8}$$

4 Discussion

Scaling. The Q^2 dependence of λ is only logarithmic. Consider first the case where the exponent of x is a constant $\lambda = \lambda_0$. Naming W_0 the function W with λ_0, equation (8) would be of the form

$$W_0(x, Q^2) = k(Q^2)^{-(1+\epsilon)} x^{-\lambda_0}, \tag{9}$$

where k is just the normalization and where we have reverted to x instead of $\bar{x}$ for simplicity, because both are equal in this kinematic domain.

In this case W_0 is a generalized homogeneous function, which, as can easily be demonstrated, implies that for all t real and bigger than zero the following equation is valid:

$$W_0(t^{-1/\lambda_0} x, t^{1/(1+\epsilon)} Q^2) = W_0(x, Q^2). \tag{10}$$

In particular, it is also valid for $t = x^{\lambda_0}$:

$$W_0|_{t=x^{\lambda_0}}(1, x^{\lambda_0/(1+\epsilon)} Q^2) \equiv W_0(\tau_0) = W_0(x, Q^2); \tag{11}$$

i.e., W_0 exhibits *exact* scaling with the scaling variable given by $\tau_0 = x^{\lambda_0/(1+\epsilon)} Q^2$.

Now, we turn to the real case where λ depends on Q^2. Using the same $t = x^{\lambda_0}$ one obtains

$$W(\tau_0) = W(x, Q^2) x^{-\delta}, \tag{12}$$

where

$$\delta \equiv \lambda_0 - \alpha \log_{10}(Q^2/\Lambda^2). \tag{13}$$

In this case the scaling is broken when δ, the exponent of x in the RHS of equation (12) is different from zero. With the help of Figure 2, note that for values of Q^2 between 1 GeV^2 and the upper limit of Q^2 used in [1], $Q^2 = 450$ GeV ^{2} (implicit for $x < 0.01$), the average value of $\lambda(Q^2)$ is close to the value of λ_{GBW}. Therefore, for $\lambda_0 = \lambda_{\text{GBW}}$ the exponent of x in the RHS of equation (12) takes its smallest values. Furthermore, one can check that for any given Q^2 in $1 < Q^2 < 450$ GeV^2, the range covered in x ($x < 0.01$) is limited in the current measured kinematic plane to an average of one order of magnitude. That means that for the given Q^2 the departure from scaling for all x points is similar and numerically small. As in the small x region $\tilde{\sigma}_{\gamma^* p} \sim \sigma_{\gamma^* p}$, this explains the approximated geometric scaling observed in [1].
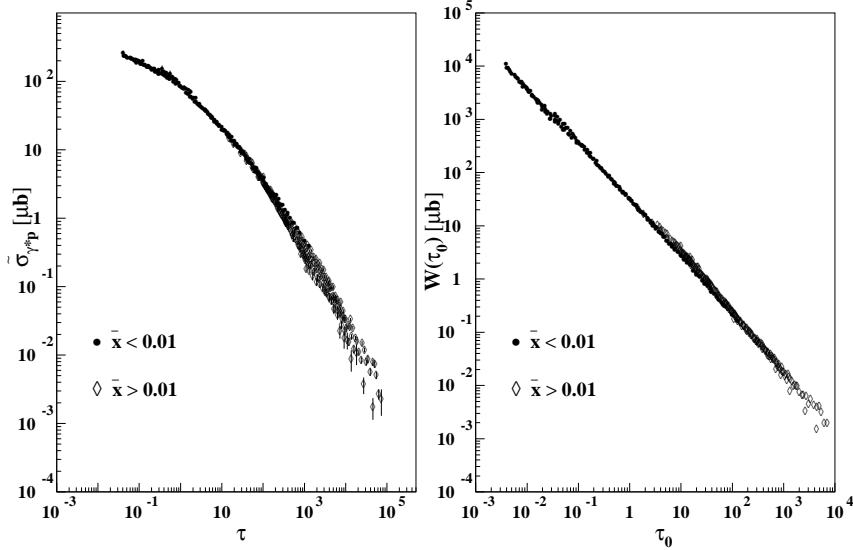
Figure 3: The left panel shows the reduced $\gamma^*\mathrm{p}$ cross section, $\tilde{\sigma}_{\gamma^*\mathrm{p}}$, as a function of the scaling variable $\tau = Q^2/Q_s^2$ [21] for all data in [27, 28, 29]. The geometric scaling behavior is clearly seen for all values of τ. The right panel shows the scaling combination of equation (12). Data points in the small x region, $x < 0.01$ are shown as full bullets to have a comparison with previous studies [1].

This argument is valid in the complete kinematic plane because, as pointed out before, for Q^2 below 1 GeV^2, W is already approximately a function of only one variable, namely x, and the data shows a smooth matching of the two behaviors. Thus, $\tilde{\sigma}_{\gamma^*\mathrm{p}}$ should display approximated geometric scaling for all values of x and Q^2.

The left panel of Figure 3 shows that this is indeed the case, while the right panel shows the scaling combination of equation (12). Note that this latter case can not be considered properly as scaling and that it is shown for illustration purposes only.

The data span some six orders of magnitude in x, and another six in Q^2. With the addition of data with $x > 0.01$ the geometric scaling behavior is extended two orders of magnitude in τ. It is quite interesting to compare Figure 3 with Figure 4. The latter figure contains all data points above $Q^2 = 1$ GeV^2 before the data collapse produced by the transformation to the scaling variable τ. The comparison of both figures shows that the collapse of all data in a single line is not a trivial fact.

Power laws, scaling and critical phenomena. It has to be emphasized that the origin of scaling within this approach is the fact that W is very close to

a generalized homogeneous function. This fact is valid even at very large values of x, where one would not necessarily expect saturation effects to be present. But it does not exclude the possibility that the mechanism which gives rise to the power law behavior of W is also linked to saturation.

In this context it is interesting to note that scaling and its relation to power laws has been widely discussed in relation to critical phenomena. In particular it has been found that under some conditions the presence of a renormalization group equation helps to explain the appearance of power laws, of its associated scaling and permits also to explain and numerically estimate the appearance of scaling violations (see for example [31, 32] and references therein).

It is interesting to note that the power law behavior of the total γ^*p cross section is generated by the branching process embodied in QCD evolution equations which are in fact a type of renormalization group equations. Also the case of saturation has been cast, within the Color Glass Condensate approach [9], in the form of renormalization group equations. It is clear then, that the subject of finding a deeper understanding of the relation between renormalization group equations and the emergence of power laws in pQCD deserves further studies.

A parametrization of $\sigma_{\gamma^*\mathrm{p}}$ above $\mathbf{Q^2 = 1\ GeV^2}$. Note that as a consequence of the description of $\sigma_{\gamma^*\mathrm{p}}$ given by equation (1) we also have a simple six parameter description of the total γ^*p cross section for *all* Q^2 values above $1\ \mathrm{GeV}^2$:

$$
\begin{aligned}
\sigma_{\gamma^*\mathrm{p}}(\bar{x}, Q^2) =& \beta \left(\frac{Q^2}{Q_0^2}\right)^{-(1+\epsilon)} \bar{x}^{-\alpha \log_{10}(Q^2/\Lambda^2)} \\
& \exp\left(-\frac{(\bar{x}-x_0)^2}{4\sigma^2}\right) \mathrm{erf}\left(\frac{1-(x-x_0)}{2\sigma}\right).
\end{aligned}
\tag{14}
$$

Equation (14) is compared to data in Figure 4 using the parameters obtained from the fit to Figure 3. For these parameters the χ^2/dof obtained for $Q^2 > 1$ GeV^2 is $\chi^2/dof = 0.77$.

5 Summary and conclusions

We have shown that $\sigma_{\gamma^*\mathrm{p}}$ can be separated as a product of a power law function, W, carrying all the information on its Q^2 evolution and a Gaussian–like distribution, V, which depends only on x. As a consequence of this *Ansatz* we obtain a six parameter description of all $\sigma_{\gamma^*\mathrm{p}}$ data above $Q^2 \approx 1\ \mathrm{GeV}^2$, where each parameter has a natural physical interpretation.

We define a reduced cross section, $W \equiv \tilde{\sigma}_{\gamma^*\mathrm{p}}$, and find that it is very close to a generalized homogeneous function over all the measured kinematic plane. This property is found to be responsible for the geometric scaling behavior of $\sigma_{\gamma^*\mathrm{p}}$ in the small x region and of $\tilde{\sigma}_{\gamma^*\mathrm{p}}$ in the complete kinematic plane. These results show that the emergence of geometric scaling is not necessary related to saturation and open up interesting possibilities for further studies of the relation between evolution equations and the appearance of scaling behavior in QCD.
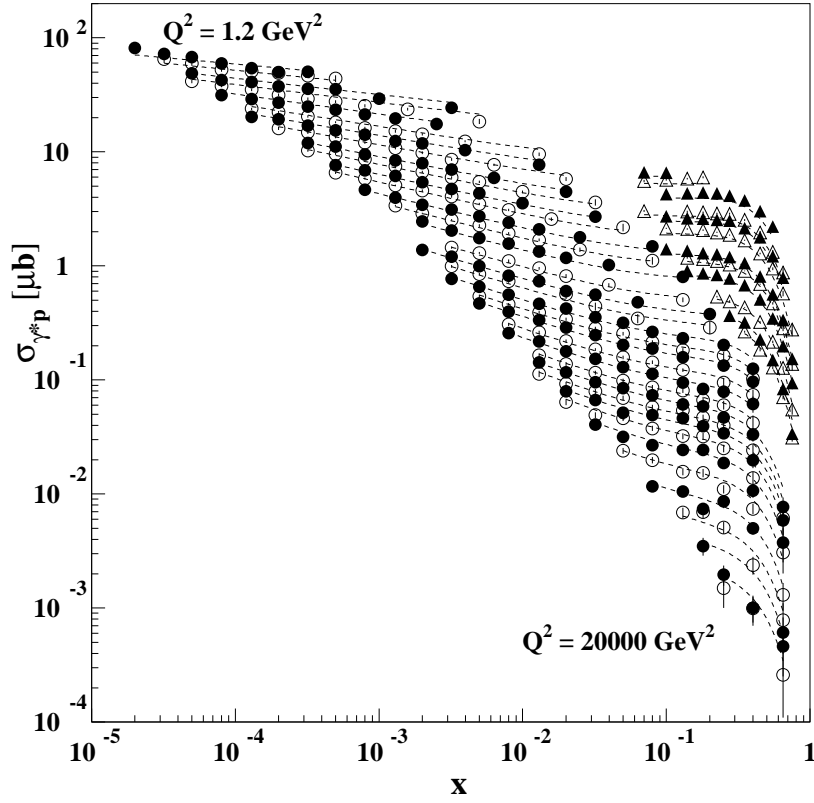
Figure 4: The total γ^*p cross section, σ_{γ^*p}, is shown as a function of x for different fixed values of Q^2 going from $Q^2 = 1.2$ GeV^2 to $Q^2 = 20000$ GeV^2. The bullets are the experimental data points from HERA, while the triangles are from fixed target experiments. The alternation of full and empty symbols is just to get a clear display of data. The lines are the result of equation (14).

References

[1] A.M. Staśto, K. Golec-Biernat and J. Kwieciński, Phys. Rev. Lett. **86**, 596 (2001).

[2] Schildknecht, B. Surrow and M. Tentyukov, Phys. Lett. B **499**, 116 (2001).

[3] A. Freund, K. Rummukainen, H. Weigert and A. Schäfer Phys. Rev. Lett. **90**, 222002 (2003).

[4] V. P. Goncalves and M.V.T. Machado, Phys. Rev. Lett. **91**, 202002 (2003).

[5] N. Armesto, C. A. Salgado and U. A. Wiedemann, Phys. Rev. Lett. **94**, 022002 (2005).

[6] L.V. Gribov, E.M. Levin and M.G. Ryskin, Phys. Rep. **100**, 1 (1983).

[7] E.M. Levin and M.G. Ryskin, Phys. Rep. **189**, 267 (1990).

[8] A.H. Mueller and J. Qiu, Nucl. Phys. B **268**, 427 (1986); J. P. Blaizot and A. H. Mueller, Nucl. Phys. B **289**, 847 (1987).

[9] L. McLerran, R. Venugopalan, Phys. Rev. D **49** 2233 (1994); **49**, 3352 (1994); **50**, 2225 (1994).

[10] I. Balitsky, Nucl. Phys. B **463**, 99 (1996).

[11] Yu. V. Kovchegov, Phys. Rev. D **60**, 034008 (1999).

[12] J. Bartels and E. Levin, Nucl. Phys. B **387**, 617 (1992).

[13] E. Levin and K. Tuchin, Nucl. Phys. B **573**, 833 (2000); Nucl. Phys. A **691**, 779 (2001); **693**, 787 (2001).

[14] E. Iancu and L. McLerran, Phys. Lett. B **510**, 145 (2001).

[15] S. Munier and R. Peschanski, Phys. Rev. Lett. **91**, 232001 (2003).

[16] E.A. Kuraev, L.N. Lipatov and V.S. Fadin, Sov. Phys. JETP **45**, 199 (1977); Ya.Ya. Balitsky and L.N. Lipatov, Sov. J. Nucl. Phys. **28**, 22 (1978).

[17] J. Kwieciński and A.M. Stásto, Phys. Rev. D **66**, 014013 (2002);

[18] E. Iancu, K. Itakura, and L. McLerran, Nucl. Phys. A **708**, 327 (2002);

[19] A.H. Mueller and D.N. Triantafyllopoulos, Nucl. Phys. B **640**, 331 (2002); D.N. Triantafyllopoulos, Nucl. Phys. B **648** 293 (2003).

[20] A. H. Mueller and A. I. Shoshi, Nucl. Phys. B **692**, 175 (2004); E. Iancu, A.H. Mueller and S. Munier, Phys. Lett. B **606**, 342 (2005).

[21] K. Golec-Biernat and M. Wüsthoff, Phys. Rev. D **59**, 014017 (1999); **60**, 114023 (1999).

[22] H1 Collab., C. Adloff *et al.*, Phys. Lett. B **520**, 183 (2001).

[23] A. de Rújula *et al.* Phys. Rev. D **10** 1649 (1974).

[24] J. Kwiecinski, J. Phys. G. **22** 685 (1996).

[25] A. Edin and G. Ingelman, Phys.Lett.B **432** 402 (1998).

[26] A. Edin and G. Ingelman, Nucl.Phys.Proc.Suppl.B **79** 189 (1999).

[27] BCDMS Collaboration, A.C. Benvenuti *et al.*, Phys. Lett. B **223**, 485 (1989).

[28] H1 Collab., C. Adloff *et al.*, Eur. Phys. J. C **19**, 269 (2001); **21**, 33 (2001); **30**, 1 (2003).

[29] ZEUS Collab, J. Breitweg *et al.*, Phys. Lett. B **487** 53 (2000).

[30] A. Donnachie and P.V. Landshoff, Phys. Lett. B **296**, 227 (1992).

[31] M. E. Fischer, Rev. Mod. Phys. **70** 653 (1998).

[32] K. G. Wilson, Rev. Mod. Phys. **55** 583 (1983).